ELSEVIER

Journal of Non-Crystalline Solids 312–314 (2002) 121–127

JOURNAL OF NON-CRYSTALLINE SOLIDS

www.elsevier.com/locate/jnoncrysol

Inelastic X-ray scattering study of the collective dynamics in simple liquid metals

T. Scopigno [a,*], U. Balucani [b], G. Ruocco [a], F. Sette [c]

[a] *Dipartimento di Fisica and INFM, Università di Roma 'La Sapienza', I-00185 Roma, Italy*
[b] *Istituto di Elettronica Quantistica CNR, I-50127 Firenze, Italy*
[c] *European Synchrotron Radiation Facility, B.P. 220, F-38043 Grenoble cedex, France*

Abstract

The collective dynamics of the so-called 'simple' liquids (in particular, liquid metals) are a good paradigm to illustrate the capabilities of inelastic X-ray scattering (IXS). In particular, it is shown how the present accuracy of the data can be exploited to provide not only a precise determination of the main spectral features (dispersion relations), but also a clue for the physical assessment of the microscopic relaxation mechanisms underlying the dynamics of the liquid state. Starting from new IXS data on liquid sodium as an example, we apply a generalized hydrodynamic framework in order to describe the details of the experimental lineshapes. A comparison with recent data on liquid lithium and aluminium is also reported: although quantitative differences indicate that the principle of corresponding states seems not to be applicable, in all these systems a simple viscoelastic approach turns out to be inadequate to reproduce the experimental data.

PACS: 61.10.Eq; 61.25.Mv; 63.50.+x

1. Introduction

As is well known, liquid metals exhibit remarkably pronounced inelastic peaks in their density fluctuations spectra up to very high Q values (well above the hydrodynamic limit), a feature that makes them ideal candidates to test different models for collective properties at finite wavevectors. For this main reason, in the last 30 years, many experimental investigations have been performed on these systems by means of inelastic neutron scattering (INS) technique, which was, up to a few years ago, the only tool adequate to investigate the dynamics of condensed matter in the mesoscopic wavevector region [1–6]. Exploiting energy conservation arguments, indeed, one infers that in the scattered spectrum an inelastic peak due to one of these excitations is well separated from the location of the incident neutron beam, and consequently its detection does not a priori involve dramatic resolution problems. This is definitely not the case for X-rays (IXS): here the energies of the incident photons are typically of order keV, i.e. 10^6–10^7 times higher than those of the excitations

* Corresponding author. Tel.: +33-4 76 88 26 03; fax: +33-4 76 88 21 60.
E-mail address: tullio.scopigno@phys.uniroma1.it (T. Scopigno).

0022-3093/02/$ - see front matter
PII: S0022-3093(02)01660-5

we are interested in. In such a case, the resolution demands clearly become quite severe. This circumstance has in fact prevented for many years an efficient and widespread use of IXS. This unfortunate situation started to improve in the 1990s which saw a substantial progress in the development of powerful and directional X-ray sources. Nowadays, the incident X-rays used in the scattering experiments are obtained from an easy-tunable, 'white' X-ray radiation produced by the so-called 'third-generation' synchrotron facilities, such as ESRF in Grenoble, APS in Argonne, SPring 8 in Japan. This positive evolution was in fact so rapid that nowadays in IXS it is possible to reach absolute energy resolutions of the order of 1 meV (namely, not very different from those typical of INS) with resolving powers higher than 10^7.

As an example of the high quality of present-day IXS data, we consider here in some detail the case of liquid sodium, lithium and aluminium which, apart from their intrinsic interest, could not be easily investigated by INS. Indeed, denoting by v the velocity of the acoustic excitation, from the conservation laws one deduces that such a Stokes spectrum is experimentally detectable only if the velocity v_{probe} of the probe used is $>v$. This restriction, clearly irrelevant in the case of electromagnetic radiation where $v_{\text{probe}} = c$, can be quite severe for neutrons. Indeed, thermal neutrons of energy ≈ 25 meV have a $v_{\text{probe}} \approx 2200$ m/s, a figure that precludes the detection of 'sound-like' inelastic peaks in many light elements, where the ordinary sound speed is very high. Moreover, the joint presence in INS of coherent and incoherent contributions to the inelastic scattering cross section, poses severe difficulties if one is interested in collective properties only.

Although through the use of INS enormous advances in the comprehension of the collective properties of condensed matter have been reported, some basic aspects remain still unsettled. In particular, due to the previously mentioned features of INS, sufficiently accurate measurements of the coherent dynamic structure factor, $S(Q,\omega)$, have hardly ever been reported, so that a quantitative description of the relaxation dynamics in monoatomic fluids was mainly based on molecular dynamic simulations rather than on real experimental data.

Recently, a number of new accurate IXS experiments have been carried out on liquid lithium and aluminium, allowing an increase in the comprehension of the relaxation processes underlying the microscopic dynamics in monoatomic fluids [7–10]. It has been possible, in fact, to detect experimentally and to quantify the presence of the relaxation scenario predicted by the theory of simple liquids: despite this 'simplicity', a number of rather complicated relaxation processes are found to affect the dynamics of these liquids. These results have been obtained within a generalized hydrodynamic approach [11,12] and following a memory function formalism [13], through a phenomenological ansatz originally proposed by Levesque et al. [14].

In this work, we report on new IXS data for the dynamic structure factor in liquid sodium at the melting point and at several fixed Q values. Within the same kind of framework already applied to lithium and aluminium, we tested the viscoelastic approximation against the experimental data discussing the number and the role of the involved relaxation processes. A comparison between the microscopic dynamics of sodium, lithium and aluminium is finally discussed.

2. The experiment

The reported data have been collected in the last three years on the IXS beamline ID16 and ID28 of the ESRF, which are now fully operative with energy resolutions of the order of $\Delta E = 1.5$ meV FWHM [15]. The experiments were always performed at fixed exchanged wavevector over a Q-region below the position of the first sharp diffraction peak. A typical energy scan ($-100 < E < 100$ meV) took about 300 min and was repeated for a total integration time of about 500 s/point. A five analyzers bench, operating in horizontal scattering geometry, allowed us to collect simultaneously photons at five different values of the exchanged wavevector Q for each single scan. As sample environment, we utilized several austenitic steel cells heated by thermal contact with a resistor

connected to a voltage regulated supply. The sample length has been always optimized by matching, as much as possible, the absorption length of the different liquids at the working energy 21 747 eV (corresponding to the Si(11 11 11) reflection in backscattering geometry).

In Fig. 1, a selection of the experimental spectra collected in a recent experiment on liquid sodium is reported as an example. Since the incident flux on the sample varies with time, the data have been normalized to the monitor. Moreover, the five analyzers have different scattering efficiencies, and so, in order to obtain the $\widetilde{S}(Q,\omega)$ in absolute units, we used the knowledge of the lower order frequency momenta of the dynamic structure factor (the tilde indicates here the true quantum dynamic structure factor, to distinguish it from its classical representation)

$$\Omega_{\tilde{S}}^{(0)} = \int \mathrm{d}\omega\, \widetilde{S}(Q,\omega) = \widetilde{S}(Q), \tag{1}$$

$$\Omega_{\tilde{S}}^{(1)} = \int \mathrm{d}\omega\, \widetilde{S}(Q,\omega)\omega = \frac{\hbar Q^2}{2M}. \tag{2}$$

Indeed, the experimental spectra, $I(Q,\omega)$, proportional to the convolution of the scattering law $\widetilde{S}(Q,\omega)$ with the resolution $R(\omega)$ is

$$I(Q,\omega) = E(Q) \int \mathrm{d}\omega'\, \widetilde{S}(Q,\omega')R(\omega-\omega'). \tag{3}$$

In terms of the lower order spectral moments of I and R: $\Omega_I^{(0)}$, $\Omega_I^{(1)}$, $\Omega_R^{(0)}$, $\Omega_R^{(1)}$ it holds that

$$\widetilde{S}(Q) = \frac{\hbar Q^2}{2M}\left(\Omega_I^{(1)}/\Omega_I^{(0)} - \Omega_R^{(1)}/\Omega_R^{(0)}\right)^{-1}. \tag{4}$$

The normalized spectra (still affected by the resolution broadening) now read

$$I_{\mathrm{N}}(Q,\omega) = \frac{\widetilde{S}(Q)}{\int I(Q,\omega)\,\mathrm{d}\omega} I(Q,\omega). \tag{5}$$

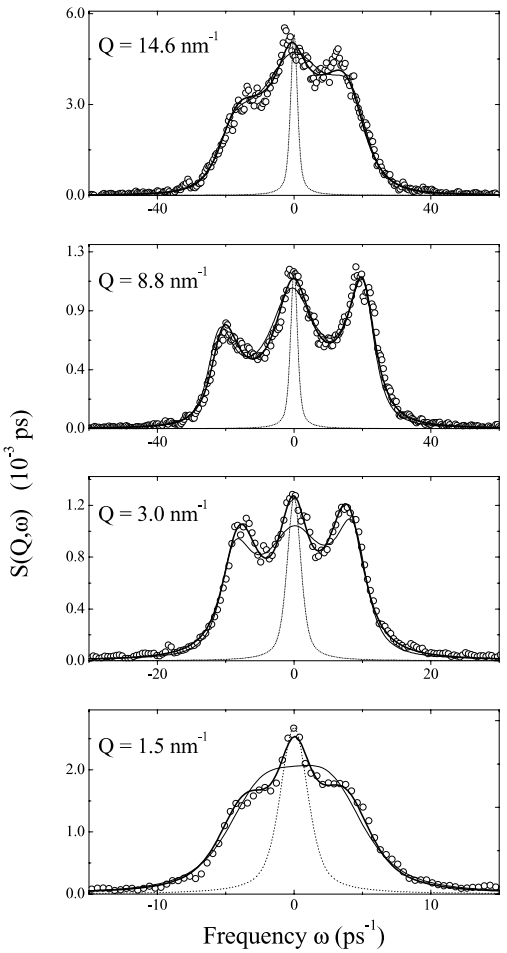

Fig. 1. Selected IXS energy spectra of liquid sodium at $T = 390$ K and fixed values of exchanged wavevector (○). Data have been normalized utilizing the sum rules according to the procedure described in the text. The best fit lineshapes with one (thin line) or two (thick line) relaxation process are also shown, along with the experimental resolution (dotted line).

3. Data analysis

The data analysis was performed following a memory function approach, discussed in more detail in Ref. [8].

Within the Langevin equation formalism, it is possible to give an expression for the *classical* dynamic structure factor in terms of the full memory function, $M(Q,t)$, which encompasses all the details of the underlying relaxation mechanisms. It can be shown that $S(Q,\omega)$ can be expressed in terms of the real and imaginary parts of $\widetilde{M}(Q,\omega)$, the Fourier transform of $M(Q,t)$ as [11]

$$\frac{S(Q,\omega)}{S(Q)} = \frac{\pi^{-1}\omega_0^2(Q)\widetilde{M}'(Q,\omega)}{\left[\omega^2 - \omega_0^2(Q) + \omega\widetilde{M}''(Q,\omega)\right]^2 + \left[\omega\widetilde{M}'(Q,\omega)\right]^2}, \tag{6}$$

where the quantity $\omega_0^2(Q) = (KTQ^2)/(mS(Q))$ is related to the generalized isothermal sound speed through the relation $c_t(Q) = \omega_0(Q)/Q$.

In order to use the above expression to reproduce the experimental spectra, $I_N(Q,\omega)$, the result (6) has to be modified to include quantum effects via the detailed balance condition and finally convoluted with the instrumental resolution, $R(\omega)$. Using one of the most common quantum recipes one finds that

$$I_N^{th}(Q,\omega) = \int \frac{\hbar\omega'/KT}{1 - e^{-\hbar\omega'/KT}} S(Q,\omega')R(\omega - \omega')\,d\omega', \tag{7}$$

which can eventually be as a fitting function to the experimental data to obtain the relevant relaxation parameters (i.e. relaxation times and strengths) by substituting in Eq. (6) the values of $\widetilde{S}(Q)$ extracted by the experimental data.

As a memory function, $M(Q,t)$, we utilized a multiple exponential ansatz. In Ref. [9], indeed, it has been shown that in a similar system, namely liquid lithium: (i) at least three distinct relaxation processes (one thermal and two viscous) are necessary to reproduce the IXS lineshape and (ii) a multi-exponential shape is an acceptable approximation of the actual memory function. Consequently the memory function reads

$$M(Q,t) = (\gamma - 1)\omega_0^2(Q)e^{-D_T Q^2 t} + \Delta^2(Q)[A(Q)e^{-t/\tau_\alpha(Q)} + (1 - A(Q))e^{-t/\tau_\mu(Q)}]. \tag{8}$$

The first term of the above equation comes from the coupling between thermal and density degrees of freedom and depends on the thermal conductivity D_T and the specific heat ratio γ. The latter two contributions are the actual viscous processes. Through the fitting procedure, the unknown parameters τ_μ, τ_α (the relaxation times), $A(Q)$ (the relative weight of the viscous processes) and $\Delta^2(Q)$ (the total viscous strength) have been deduced.

In Fig. 1, we report the outcome of the fitting procedure, i.e. a comparison between $I_N^{th}(Q,\omega)$ and $I_N(Q,\omega)$. Initially, a one-relaxation-time ansatz (viscoelastic model) has been tried. In fact, albeit being a simple approximation for $M(Q,t)$, the viscoelastic model is found to account rather well for many features of the collective dynamics detected in the measurements. Taking an experimentalist's point of view, one may wonder if it is really worthwhile to proceed further. Another face of the same coin is whether the experimental data themselves are sufficiently accurate to deserve a more refined treatment. Since a few years ago, the analysis of collective dynamics data was in fact performed in terms of the viscoelastic model (or even simpler versions of it, such as the 'damped harmonic oscillator' model). As an example, consider one of the most accurate INS experiments performed in a simple liquid, cesium just above the melting point [5]. The location of the inelastic peak and the occurrence at finite Q of a positive dispersion (effective speed of sound larger than the ordinary hydrodynamic value) can be established rather well. Yet, despite the efforts of the authors, any check of possible discrepancies of the viscoelastic model was prevented by the limited accuracy of the data at low frequencies. Such a situation is of course bound to change as a result of the evolution in the instrumentation. This is exactly what happened in IXS. Even a few years ago, the relatively low energy resolution of IXS experiments (>10 meV) permitted only the location of the positions of (possible) inelastic peaks [16,17]. Nowadays, the resolution is improved to such an extent to yield in many cases a rather accurate determination of the spectral shape of the dynamic structure factor. Indeed, a one-relaxation-time description (viscoelastic model) turns out to be untenable for an accurate reproduction of the data. In particular at low Qs the joining contribution of two processes is crucial even to catch the qualitative features of the spectra only, as clearly shown in Fig. 1.

In Fig. 2 we show the two relaxation times, τ_α and τ_μ, as obtained by the fitting procedure. The timescale of the slower (α) process is almost wavevector independent, with an abrupt increase below $Q \approx 6$ nm^{-1}. Such an increase is probably an artifact, as it occurs as the timescale approaches the inverse of the resolution width, here reported as a dashed line. Consequently the determination

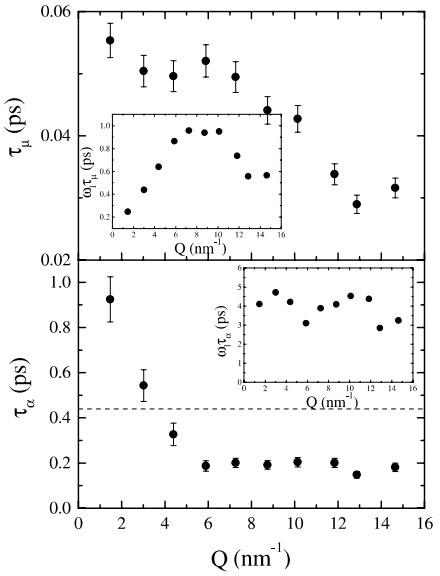

Fig. 2. Main frame: Fast and slow relaxation times as obtained by the fitting procedure. Inset: Product of the relaxation times and the position of the inelastic peak of the classical density correlation function, as deduced by the fit.

of the α relaxation time below this Q value is no longer reliable. The microscopic (μ) relaxation process shows instead slightly decreasing Q dependence. In the insets of Fig. 2, the $\omega\tau$ values are reported as function of Q for the two processes (ω is here the dominant frequency of the density fluctuations measured at a given Q, i.e. the frequency of the Brillouin component). These quantities give important indications about the role of the two processes. The faster one, indeed, has values of $\omega\tau$ always smaller than 1, so that it is mainly responsible for the acoustic damping (Brillouin linewidth). Moreover, $\omega(Q)\tau_\mu(Q)$ shows an increase in the same region where the sound dispersion occurs (below the position of the one half of the first sharp diffraction peak), so that an increase of the apparent peak frequency ruled by the strength of the fast process has to be expected. The $\omega(Q)\tau_\alpha(Q)$ is always larger than 1. Consequently the α process mainly controls the sharper portion of the quasielastic scattering, while it only gives a slight contribution to the speed of sound all over the explored Q range (the strength of the α process is negligible with respect to the one of the fast relaxation).

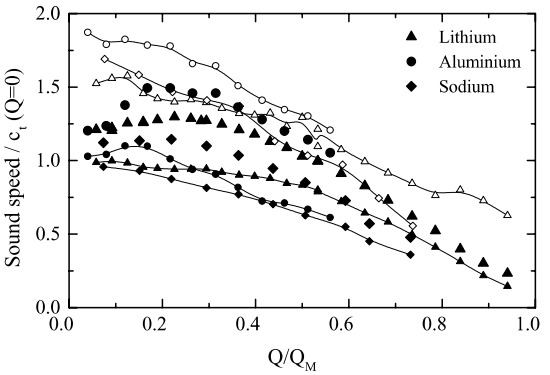

Fig. 3. Apparent sound speed (large full symbols) compared to the low frequency, isothermal, behavior (small full symbols + guideline). The instantaneous value $c_\infty(Q)$ is also reported (small open symbols + guideline).

The above mentioned increase of the speed of sound in the different systems we investigated is shown in Fig. 3 which reports $\omega_l(Q)/Q$, the apparent sound velocity deduced by the maximum of the longitudinal current correlation spectrum $J^L(Q,\omega) = (\omega^2/Q^2)S(Q,\omega)$. We always find that the isothermal value of the sound speed is not yet reached at the minimum wavevector probed in our experiments (about 1.0 nm^{-1}). In the case of sodium, this seems to contradict earlier results [18]. It is worth to point out that at low Qs resolution effects are particularly important (and sodium is the most critical sample in this sense, being the one with the lower sound speed); even with the present resolution (1.5 meV FWHM) the Brillouin components of the $S(Q,\omega)$ appear as shoulders of the quasielastic signal (see Fig. 1), therefore we believe that this discrepancy may be ascribed to the lower resolutions of the previous experiment which prevented an accurate determination of the actual lineshape at such small Q value. Both the isothermal $c_t(Q)$ (low frequency) [1] and the infinite frequency $c_\infty(Q)$ values of the sound speed have

[1] Due to the high thermal conductivity of liquid metals as compared to ordinary fluids, the crossover in the sound speed associated with the thermal relaxation occurs well below 1 nm^{-1}, approximatively the lower Q accessible to IXS. Consequently in the IXS window the low frequency limits of the sound speed is the isothermal rather than the adiabatic sound speed [8].

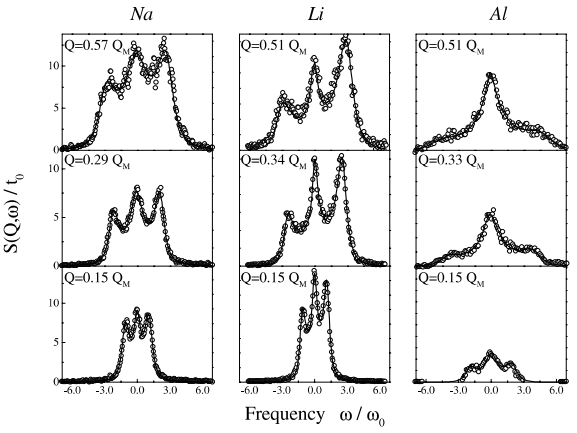

Fig. 4. Comparison of the IXS spectra of sodium, lithium and aluminium reported in scaled units as defined in the text. Best fit lineshape (two time-relaxation model) are also shown.

been reported as obtained by the fit. This latter quantity is higher than the maximum value reached by the apparent sound speed; this is due partially to the fact that the μ process never reaches a fully unrelaxed regime ($\omega\tau \gg 1$) and partially to the oversimplified assumption about the exponential nature of the relaxation [8].

We conclude this investigation with the direct comparison of $S(Q,\omega)$ in three different liquid metals. In Fig. 4 we report a comparison between the IXS data on liquid sodium with lithium and aluminium. To compare these three different systems, one can define an absolute common scale introducing a set of length, mass and time units $[l^*, m^*, t^*]$ for each system, a procedure that can be considered exact up to the extent of validity of the corresponding states principle (holding at equal values of reduced density and temperature). As a length unit, l^*, we have chosen $l^* = Q_m^{-1}$, the inverse of the position of the static structure factor $S(Q)$. The time unit, t^*, has been chosen instead as $t^* = \sqrt{m/T_m}\,l$ with T_m the melting temperature; finally, m^* is the atomic mass. In the upper panel the raw IXS signal, measured by these units is reported. The Q values have been selected to be as close as possible for three different regions of the dispersion curve. The aluminium spectra clearly have a different lineshape, while lithium and sodium are much more similar in their respective absolute units. This notwithstanding, the lineshapes of the two alkali systems do not coincide, and we conclude that the principle of corresponding state does not apply to these systems, as one could expect by the numerical differences observed in the behavior of the apparent sound speed.

4. Conclusions

In this contribution, we have tried to show the maturity of IXS as a valuable and accurate tool to investigate the collective dynamics of condensed matter. In this area, the statement that a judicious use of both IXS and INS leads to important advances, rather than sounding pretentious, is nowadays widely accepted. In this respect, the analysis of the IXS data in liquid sodium, lithium and aluminium is a good example. Besides revealing the inadequacies of the viscoelastic model, its main merit lies in the fact that the results are one of the first experimental evidences of the two-timescale processes predicted by kinetic and mode-coupling approaches in the last decade or so [19]. In these theories, the memory function $M(Q,t)$ is predicted to decrease from its initial $t = 0$ value by a very fast decay mechanism (characteristic times 10^{-13} s), which stems from interactions quite localized both in space and in time. These interactions are often identified with the same 'uncorrelated' collisional events typical of the kinetic theory of gases, where the above timescale measures the duration of a collision. Although this is the most common interpretation, other explanations of this fast mechanism have been proposed [8,20,21]. The fast microscopic mechanism is thought to be the only one present in a dilute fluid, but at increasing particle densities, the assumption that two subsequent collisions are uncorrelated becomes doubtful; memory effects gradually emerge, with typical times considerably longer ($\approx$1–10 ps for an ordinary liquid) than the previous timescale. The nature of the processes causing this long-lasting tails strongly depends on the density and the temperature. At increasing densities and/or decreasing temperatures, the particles have a lower mobility, and a process referred to as structural relaxation becomes dominant. Although the mechanisms ruling out the dynamics of the three different systems turn out to

lie in a same general framework, important quantitative differences have been reported. In particular the scaling law that the principle of corresponding state would predict seems not to hold.

Acknowledgements

One of the authors (T.S.) would like to thank R. Yulmetyev and M. Silbert for stimulating discussions.

References

[1] J.R.D. Copley, M. Rowe, Phys. Rev. A 9 (1974) 1656.
[2] P. Verkerk, P.H.K. De Jong, M. Arai, S.M. Bennington, W.S. Howells, A.D. Taylor, Physica B 180&181 (1992) 834.
[3] P.D. Randolph, Phys. Lett. 3 (1963) 162;
C. Morkel, W. Glaser, Phys. Rev. A 33 (1986) 3383;
A. Stangl, C. Morkel, U. Balucani, A. Torcini, J. Non-Cryst. Solids 205–207 (1996) 402.
[4] A.G. Novikov, V.V. Savostin, A.L. Shimkevich, R.M. Yulmetyev, Physica B 228 (1996) 312.
[5] T. Bodensteiner, C. Morkel, W. Gläser, B. Dorner, Phys. Rev. A 45 (1992) 5709.
[6] P. Chieux, J. Dupuy-Philon, J.F. Jal, J.B. Suck, J. Non-Cryst. Solids 205–207 (1996) 370.
[7] T. Scopigno, U. Balucani, A. Cunsolo, C. Masciovecchio, G. Ruocco, F. Sette, R. Verbeni, Europhys. Lett. 50 (2000) 189.
[8] T. Scopigno, U. Balucani, G. Ruocco, F. Sette, J. Phys. C 12 (2000) 8009.
[9] T. Scopigno, U. Balucani, G. Ruocco, F. Sette, Phys. Rev. Lett. 85 (2000) 4076.
[10] T. Scopigno, U. Balucani, G. Ruocco, F. Sette, Phys. Rev. E 63 (2001) 011210.
[11] U. Balucani, M. Zoppi, Dynamics of the Liquid State, Clarendon, Oxford, 1983.
[12] J.P. Boon, S. Yip, Molecular Hydrodynamics, McGraw-Hill, New York, 1980.
[13] H. Mori, Prog. Theor. Phys. 33 (1965) 423.
[14] D. Levesque, J. Verlet, J. Kurkijarvi, Phys. Rev. A 7 (1973) 1690.
[15] C. Masciovecchio, U. Bergman, M. Krisch, G. Ruocco, F. Sette, R. Verbeni, Nucl. Instrum. and Meth. B 111 (1986) 181, 117 (1986) 339.
[16] E. Burkel, Inelastic Scattering of X-rays with Very High Energy Resolution, Springer, Berlin, 1991;
E. Burkel, H. Sinn, J. Phys.: Condens. Matter 6 (1994) A225;
E. Burkel, H. Sinn, Int. J. Thermophys. 16 (1995) 1135.
[17] H. Sinn, F. Sette, U. Bergmann, Ch. Halcousis, M. Krisch, R. Verbeni, E. Burkel, Phys. Rev. Lett. 78 (1997) 1715.
[18] W.C. Pilgrim, S. Hosokawa, H. Saggau, H. Sinn, E. Burkel, J. Non-Cryst. Solids 250–252 (1999) 96.
[19] L. Sjogren, Phys. Rev. A 22 (1980) 2866, 2883.
[20] G. Ruocco, F. Sette, R. Di Leonardo, G. Monaco, M. Sampoli, T. Scopigno, G. Viliani, Phys. Rev. Lett. 84 (2000) 5788.
[21] T. Scopigno, G. Ruocco, F. Sette, G. Viliani, Phys. Rev. E 66 (2002), in press.